Rapid Communications

Controlling stability and emergent rotation of the skyrmion crystal in thin films of helimagnets via tilted magnetic field

Xuejin Wan, Yangfan Hu,* and Biao Wang†

Sino-French Institute of Nuclear Engineering and Technology, Sun Yat-sen University, 519082, Zhuhai, China

(Received 1 March 2019; revised manuscript received 16 April 2019; published 10 May 2019)

The interaction of a tilted magnetic field and the intrinsic anisotropy of magnetic thin films leads to profound effects on the deformation, orientation, and stability of the skyrmion crystal (SkX) phase, which has yet to be explored comprehensively. Here, we study the combined effects of a tilted magnetic field and the exchange anisotropy on SkX in thin films of helimagnets. By applying an analytical framework suitable for deformed or rotated SkX, not only the strength of the magnetic field but also the polar angle and the azimuthal angle, which describe the direction of the magnetic field, are found to affect the stability of SkX. Moreover, they reorientate SkX at certain conditions. Our findings pave a way for the manipulation of SkX.

DOI: 10.1103/PhysRevB.99.180406

Introduction. Magnetic skyrmions are topologically protected emergent particles, which have a nontrivial spin texture with opposite magnetization directions at the center and the edge. In helimagnets with broken spatial inversion symmetry [1–15] or in interfacially asymmetric multilayers [16–18], skyrmions can be stabilized by the Dzyaloshinskii-Moriya interaction (DMI) in varies states, including the skyrmion crystal (SkX) phase, skyrmion glass [5], skyrmion clusters [9], and isolated skyrmions. Due to their small size, high robustness, and facile current driven motion [19,20], skyrmions have great potential in the next generation spintronic devices. Skyrmion-based storage devices, logic gates [21], and racetrack memories [22] can be expected to have a high memory density and suffer less from the Joule heat.

Since the experimental discovery of skyrmions in helimagnets, their manipulation has attracted growing scientific interest. Various external fields were applied to control the stability, deformation, motion, and excitation of skyrmions [7,23–34]. As an important ingredient for the manipulation of skyrmions, a magnetic field is widely considered in the studies of skyrmions in helimagnets. Different kinds of magnetic fields, including oscillating [30], pulse [31], and static fields, and uniform and gradient fields [32], have been applied to investigate the responses of skyrmions, where the magnetic field is mostly applied perpendicular to the skyrmion plane. In the several cases where a tilted magnetic field [26,29,35–40] is considered, the effect of the azimuthal angle, which characterizes the in-plane direction of the magnetic field, is not discussed.

When isolated skyrmions condense to SkX, their in-plane axial symmetry is reduced to hexagonal symmetry [41]. As a result, the orientation of SkX will be affected by the azimuthal angle of a tilted magnetic field. Furthermore, if the intrinsic anisotropy of helimagnets, e.g., exchange anisotropy [42], is considered, the interplay between intrinsic in-plane anisotropy and anisotropy of a magnetic field will result in complex direction-related effects on SkX. Not only the orientation but also the stability of SkX are expected to be affected by the azimuthal angle. Thus, the azimuthal angle of a tilted magnetic field may have a significant effect on the SkX, which may lead to an effective approach to manipulating SkX.

SkX stabilized in a tilted magnetic field consists of two types: Néel SkX or anti-SkX in bulk polar magnets [35–40], and Bloch SkX in thin films of helimagnets [26,29]. In this Rapid Communication, we focus on the latter type, and study the combined effects of a tilted magnetic field and the exchange anisotropy on Bloch SkX in films of helimagnets. We apply a continuous free-energy-density model with exchange anisotropy included and describe SkX by a Fourier expansion with deformation-related degrees of freedom [42,43]. Via minimization of free-energy density, we obtain the analytical expressions for different magnetic phases, including the helical phase, ferromagnetic phase, and SkX. Here, the conical phase is not considered, because in thin films of helimagnets with a sufficiently small thickness (less than the period of the conical phase), the conical phase is suppressed [6]. By plotting the phase diagrams, we find that the stable region of SkX in the phase diagram varies with both the polar and azimuthal angles. To investigate the rotation of SkX under a tilted magnetic field, we first consider separately the effects of a tilted magnetic field and the effects of the exchange anisotropy, and we find that a tilted magnetic field tends to orientate SkX with one of the wave vectors along its in-plane component, while exchange anisotropy tends to orientate SkX with one of the wave vectors along the x or y axis. When both the tilted magnetic field and the exchange anisotropy are considered, directional effects arise, and all the three parameters describing a tilted magnetic field, its strength, polar angle, and azimuthal angle, can rotate SkX.

*Corresponding authors: huyf3@mail.sysu.edu.cn
†wangbiao@mail.sysu.edu.cn

Methods. We use the rescaled free-energy density [42]

$$\widetilde{\omega}(\mathbf{m}) = \sum_{i=1}^{3}\left(\frac{\partial \mathbf{m}}{\partial r_i}\right)^2 + 2\mathbf{m}\cdot(\nabla\times\mathbf{m}) - 2\mathbf{b}\cdot\mathbf{m} + t\mathbf{m}^2 + \mathbf{m}^4 + a_{\mathrm{e}}\sum_{i=1}^{3}\left(\frac{\partial m_i}{\partial r_i}\right)^2. \quad (1)$$

Here, the magnetization $\mathbf{m}$ is chosen as the three-dimensional order parameter field. The first two terms in Eq. (1) represent, respectively, the exchange interaction and the DMI. The third term is the Zeeman coupling to an external magnetic field $\mathbf{b} = b[\cos\varphi\sin\theta, \sin\varphi\sin\theta, \cos\theta]^{\mathrm{T}}$ (θ and φ are the polar angle and azimuthal angle in the spherical coordinates, respectively). $t\mathbf{m}^2 + \mathbf{m}^4$ consists of the second- and fourth-order terms of Landau expansion with rescaled temperature t. The last term is the exchange anisotropy with coefficient a_{e}.

As to the mathematical description for the magnetization texture in helimagnet thin films, we apply the following n-order Fourier representation,

$$\mathbf{m} = \mathbf{m}_0 + \sum_{i=1}^{n}\sum_{j=1}^{n_i}\mathbf{m}_{\mathbf{q}_{ij}} e^{i\mathbf{q}_{ij}^d\cdot\mathbf{r}}. \quad (2)$$

Here, $\mathbf{m}_0 = [m_{01}, m_{02}, m_{03}]^{\mathrm{T}}$ is the averaged magnetization, and n_i stands for the number of ith-order waves which have the same wavelength (see Ref. [41] for values of some n_i). $\mathbf{q}_{ij}$ ($j = 1, 2, \ldots, n_i$) are the ith-order undeformed wave vectors, which can be seen as vectors of the reciprocal lattice spanned by the basis $\mathbf{q}_{11}$ and $\mathbf{q}_{12}$. Without loss of generality, for hexagonal SkX, we set $\mathbf{q}_{11} = [0, 1]^{\mathrm{T}}$ and $\mathbf{q}_{12} = [-\frac{\sqrt{3}}{2}, -\frac{1}{2}]^{\mathrm{T}}$. $\mathbf{q}_{ij}^d$ ($j = 1, 2, \ldots, n_i$) are the ith-order deformed wave vectors, and they are related to the undeformed wave vectors by

$$\mathbf{q}_{ij}^d = \begin{bmatrix} 1+\varepsilon_{11}^q & \varepsilon_{12}^q + \omega^q \\ \varepsilon_{12}^q - \omega^q & 1+\varepsilon_{22}^q \end{bmatrix}\mathbf{q}_{ij}, \quad (3)$$

where ε_{11}^q, ε_{22}^q, ε_{12}^q, and ω^q are parameters reflecting the shape deformation of the SkX. In reciprocal space, ε_{11}^q and ε_{22}^q account for the elongation of the x axis and y axis; ε_{12}^q and ω^q account for the shear deformation and rotation of the xy plane. $\mathbf{m}_{\mathbf{q}_{ij}}$ denotes the wave polarization. With $\mathbf{P}_{ij1} = \frac{1}{\sqrt{2}|\mathbf{q}_{ij}|}[-iq_{ijy}, iq_{ijx}, |\mathbf{q}_{ij}|]^{\mathrm{T}}$, $\mathbf{P}_{ij2} = \frac{1}{|\mathbf{q}_{ij}|}[q_{ijx}, q_{ijy}, 0]^{\mathrm{T}}$, and $\mathbf{P}_{ij3} = \frac{1}{\sqrt{2}|\mathbf{q}_{ij}|}[iq_{ijy}, -iq_{ijx}, |\mathbf{q}_{ij}|]^{\mathrm{T}}$ as the orthonormal basis, $\mathbf{m}_{\mathbf{q}_{ij}}$ can be expressed in the following form,

$$\mathbf{m}_{\mathbf{q}_{ij}} = \sum_{k=1}^{3} c_{ijk}\mathbf{P}_{ijk}, \quad (4)$$

where $c_{ijk} = c_{ijk}^{\mathrm{re}} + ic_{ijk}^{\mathrm{im}}$ ($k = 1, 2, 3$) are the complex expansion coefficients.

For undeformed SkX with hexagonal symmetry, we have the following restrictions on c_{ijk},

$$c_{ijk} = c_{ilk} \quad (\mathbf{q}_{ij} + \mathbf{q}_{il} \neq \mathbf{0}), \quad (5a)$$

$$c_{ijk} = c_{ilk}^* \quad (\mathbf{q}_{ij} + \mathbf{q}_{il} = \mathbf{0}), \quad (5b)$$

while, for deformed SkX, the restrictions Eq. (5a) should be discarded. As a result, $7 + \sum_{i=1}^{n} 3n_i$ parameters are needed to describe the SkX magnetization texture. They are the shape-related ones ε_{11}^q, ε_{22}^q, ε_{12}^q, ω^q, and the internal-structure-related ones, m_{01}, m_{02}, m_{03}, c_{ijk}^{re}, c_{ijk}^{im} ($i = 1, 2, \ldots, n$; $j = 1, 2, \ldots, \frac{n_i}{2}$; $k = 1, 2, 3$). Here, we chose $\mathbf{q}_{ij} = -\mathbf{q}_{il}$ for $l = j + \frac{n_i}{2}$; therefore, $c_{ijk} = c_{i(j+n_i/2)k}^*$. At fixed temperature t, applied tilted magnetic field $\mathbf{b}$, and exchange anisotropy a_{e}, these parameters are obtained via minimization of the rescaled free-energy-density Eq. (1). Here, we chose the order of Fourier expansion $n = 3$ [42]. It should be emphasized that Eq. (2) can be used to describe not only the deformed (or undeformed) SkX but also the helical phase and ferromagnetic phase. For the helical phase, the coefficients c_{ijk} are nonzero only along one certain $\mathbf{q}_{ij}$ direction; for the ferromagnetic phase, c_{ijk} are all zero.

Stability of SkX. It has been shown by Monte Carlo simulation that the stability of Bloch SkX in thin films depends on the polar angle of a tilted magnetic field [26,29]. In these simulation works, due to the necessary discretization step, the anisotropic energy which resembles the crystal field anisotropy in real materials arises naturally. This means that in-plane directions are not all equivalent. Therefore, the azimuthal angle characterizing the direction of anisotropy induced by a magnetic field will play an important role in the behaviors of SkX. Regretfully, no attention has been paid to it. Different from the simulation method, the model we applied is a continuous one in Eq. (1) with exchange anisotropy considered. We set the rescaled exchange anisotropy coefficient $a_{\mathrm{e}} = -0.05$, and first study the effects of azimuthal and polar angles on SkX stability. At different b, t, θ, and φ, we solve the equilibrium state by minimizing the averaged free energy. Some of the results are plotted in the phase diagrams of Fig. 1.

For a fixed polar angle $\theta = 50^\circ$, the azimuthal angle has a noticeable influence on the stability of SkX. As shown in Figs. 1(a)–1(c), with increasing azimuthal angle φ, the area of the region where SkX exists as an equilibrium state decreases and reaches its minimum at $\varphi = 45^\circ$ (we need not consider the interval $45^\circ \leqslant \varphi \leqslant 90^\circ$, because the exchange anisotropy permits the equivalence of the x and y axes). It can be also found that the helical phase is stable in two separate regions in the phase diagrams: The major one is at a low magnetic field and the minor one is at a high magnetic field. By increasing the magnetic field, we expect to observe the phase transitions from the helical phase to SkX then back to the helical phase and finally at a sufficient high magnetic field to ferromagnetic phase. A similar phenomenon has been observed in FeGe film [27].

Figures 1(d) and 1(e), together with Fig. 1(c), show the influence of the polar angle on the stability of SkX. It can be concluded that a lower polar angle favors SkX. This agrees with the Monte Carlo simulation results [26]. By comparing Figs. 1(d) and 1(e), we find that the difference between the phase diagrams at $\theta = 25^\circ$ and $\theta = 0^\circ$ is not so obvious. While this is not the case for the phase diagrams at $\theta = 50^\circ$ and $\theta = 25^\circ$, the stable region of SkX in Fig. 1(c) is much smaller than that in Fig. 1(d). Moreover, at a low polar angle, the helical phase at high magnetic field disappears. To work this out, we draw the b-θ phase diagram at the azimuthal angle $\varphi = 45^\circ$ in Fig. 1(f). It is found that the phase transition line between the ferromagnetic phase and SkX is almost horizontal, meaning that the azimuthal angle does not influence so

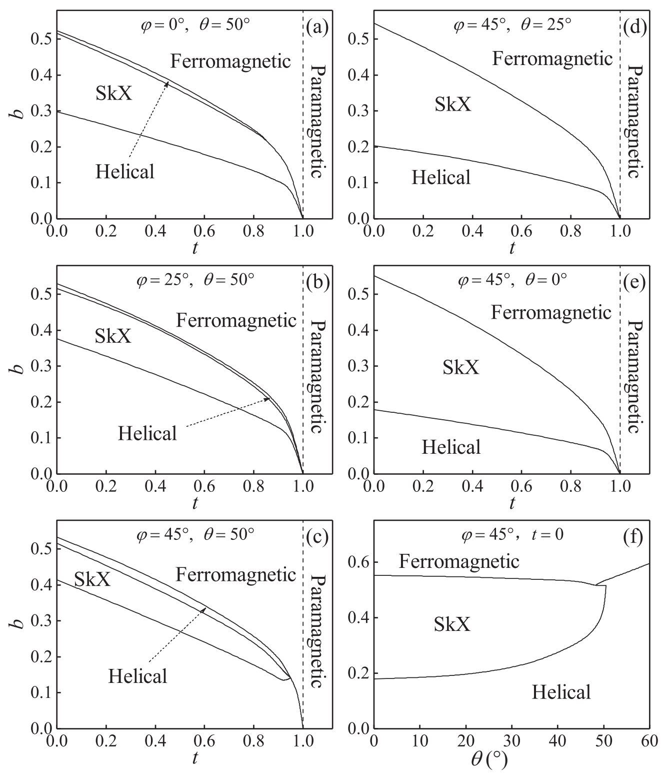

FIG. 1. (a)–(c) Magnetic field-temperature (b-t) phase diagrams at the same polar angle $\theta = 50°$ and different azimuthal angles of the tilted magnetic field. (d) and (e) b-t phase diagrams at the same azimuthal angle $\varphi = 45°$ and different polar angles. (f) Magnetic field-polar angle (b-θ) phase diagram at the temperature $t = 0$ and the azimuthal angle $\varphi = 45°$.

much the phase transition between SkX and the ferromagnetic phase. With increasing polar angle, the threshold value of the magnetic field for the phase transition between the helical phase and SkX increases slowly at low θ, while sharply at high θ, especially when θ is about 50°. The high-field helical phase appears at about $\theta = 48°$. Figure 2 shows the critical angle θ_c, for which SkX disappears totally in the phase diagram, as a function of the exchange anisotropy. θ_c varies almost lineally with a_e from about 34° ($a_e = -0.8$) to about 52° ($a_e = 0$). The value of θ_c for zero exchange anisotropy is between 50° in Ref. [29] and 60° in Ref. [26] obtained by Monte Carlo simulation.

Rotation of SkX. A magnetic field with nonzero tilt angle will induce anisotropic Zeeman energy and thus break the

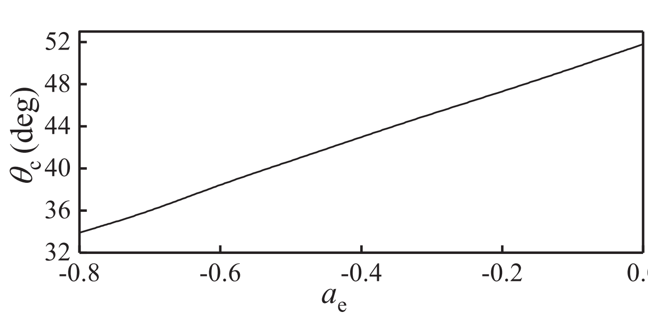

FIG. 2. θ_c as a function of a_e at $t = 0$ and $\varphi = 45°$.

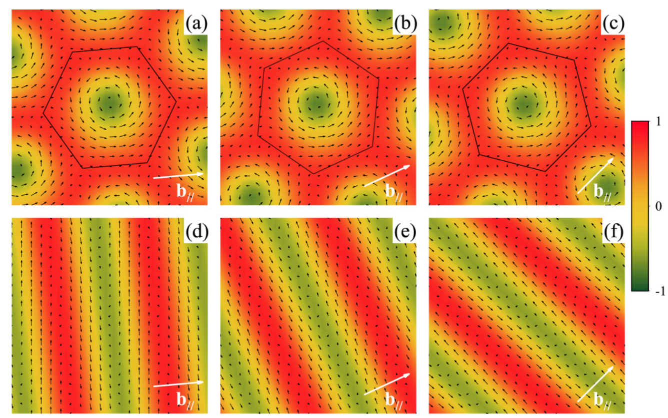

FIG. 3. Magnetization structure of SkX and helical phase at $t = 0$, $a_e = 0$, and $\theta = 30°$. SkX and the helical phase are stabilized at $b = 0.4$ and $b = 0.1$, respectively. The chosen azimuthal angles are 5° for (a) and (d), 25° for (b) and (e), and 45° for (c) and (f). The distributions of the in-plane and out-of-plane components of magnetization are represented respectively by the black arrows and the colored density plot. The skyrmion Wigner-Seitz cells are encircled by the hexagons. The white arrow stands for the direction of $\mathbf{b}_\parallel$, which is the projection of the magnetic field onto the film plane.

symmetry of the free-energy density. Intuitively, a periodic magnetization structure has a certain orientation preference in such a tilted magnetic field. To prove this, we ignore the effects of the other anisotropies, and calculate the magnetization structures of SkX and helical phase at different azimuthal angles. Figures 3(a)–3(c) [Figs. 3(d)–3(f)] show the reorientation of SkX (helical phase) with respect to the azimuthal angle at the conditions $t = 0$, $a_e = 0$, $\theta = 30°$, and $b = 0.4$ ($b = 0.1$). Without considering the intrinsic anisotropies or other induced anisotropies, the wave vector of the helical phase or SkX tends to be aligned with the in-plane component of the tilted magnetic field.

Let us now consider the case with exchange anisotropy coefficient a_e set to be -0.05. When the magnetic field is normal to the thin-film plane, the helical phase is orientated with the wave vector along a $\langle 11 \rangle$ direction, while SkX is orientated with one of the wave vectors along a $\langle 10 \rangle$ direction. For a tilted magnetic field, we calculate the magnetization structures of the helical phase and SkX at different azimuthal angles and plot the results in Fig. 4, which has the same temperature and magnetic field conditions as Fig. 3. When $\mathbf{b}_\parallel$, the projection of the magnetic field onto the film plane, is along the [11] direction [Fig. 4(f)], the helical wave vector is aligned with the direction $\mathbf{b}_\parallel$. When $\mathbf{b}_\parallel$ is not along the [11] direction [Figs. 4(d) and 4(e)], the anisotropy of the magnetic field and the exchange anisotropy compete with each other, resulting in the deviation of the helical wave vector from the [11] direction. The situation for SkX is more complicated. For the azimuthal angle near 0°, one of the wave vectors tends to align with the y axis, while for the azimuthal angle near 45°, one of the wave vectors tends to align with $\mathbf{b}_\parallel$.

To further study the reorientation effects of combined anisotropies on SkX, we plot φ_{11} and φ_{12}, the direction angles of $\mathbf{q}^d_{11}$ and $\mathbf{q}^d_{12}$, as functions of the azimuthal angle φ in

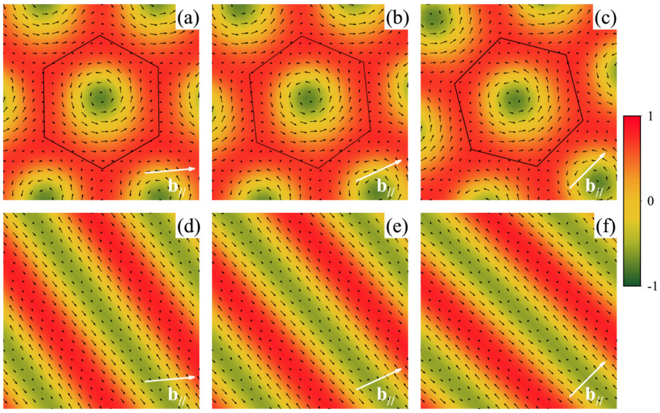

FIG. 4. Magnetization structure of SkX and helical phase at $t = 0$, $a_e = -0.05$, and $\theta = 30^\circ$. SkX and the helical phase are stabilized at $b = 0.4$ and $b = 0.1$, respectively. The chosen azimuthal angles are 5° for (a) and (d), for 25° (b) and (e), and 45° for (c) and (f).

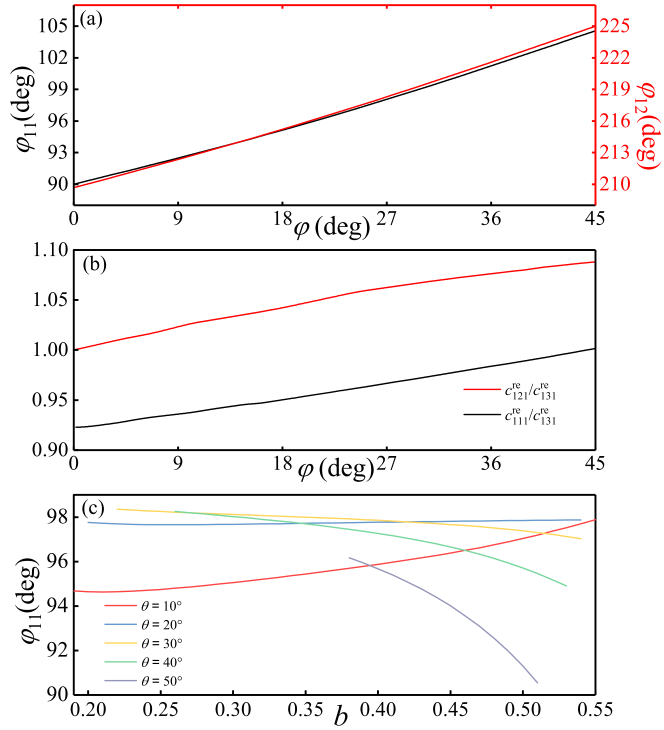

FIG. 5. (a) φ_{11} and φ_{12} as functions of φ at $t = 0$, $b = 0.5$, $a_e = -0.05$, and $\theta = 30^\circ$. (b) The relative wave amplitudes $c^{re}_{121}/c^{re}_{131}$ and $c^{re}_{111}/c^{re}_{131}$ as functions of φ at $t = 0$, $b = 0.5$, $a_e = -0.05$, and $\theta = 30^\circ$. (c) φ_{11} as a function of b at $t = 0$, $\varphi = 25^\circ$, $a_e = -0.05$, and at different θ.

Fig. 5(a). At $\varphi = 0^\circ$, φ_{11} is exactly 90°, thus $\mathbf{q}^d_{11}$ is along the y axis; at $\varphi = 45^\circ$, φ_{12} is exactly 225°, thus $\mathbf{q}^d_{12}$ is along the [11] direction. By increasing φ from 0° to 45°, φ_{11} increases smoothly from 90° to about 105°, and φ_{12} increases smoothly from about 210° to 225°. This means that SkX is driven to rotate along the z axis about 15° by a tilted magnetic field. Due to the equivalence of the x and y axes, if we continue to increase the azimuthal angle to 90°, SkX is expected to rotate continuously to the final state with a wave vector along the x axis. Figure 5(b) shows the dominant Fourier coefficients as functions of the azimuthal angle. The inequality of c^{re}_{111}, c^{re}_{121}, and c^{re}_{131} implies that a tilted magnetic field with the interplay of exchange anisotropy distorts the hexagonal skyrmion lattice. At $\varphi = 0^\circ$, we have $c^{re}_{121} = c^{re}_{131}$; in this case, $\mathbf{q}^d_{12}$ and $\mathbf{q}^d_{13}$ waves are equivalent; at $\varphi = 45^\circ$, we have $c^{re}_{111} = c^{re}_{131}$; in this case, $\mathbf{q}^d_{11}$ and $\mathbf{q}^d_{13}$ waves are equivalent. From the viewpoint of symmetry, the results are reasonable. When the in-plane component of a magnetic field is parallel to the axes with high symmetry, [11] and [10], the waves in the Fourier representation Eq. (2) are expected to be symmetric with respect to these axes. This may partly explain the behaviors of SkX driven by a tilted magnetic field.

Finally, we discuss the effects of magnetic field strength b and polar angle on SkX rotation. We set the azimuthal angle $\varphi = 25^\circ$, the temperature $t = 0$, the exchange anisotropy coefficient $a_e = -0.05$, and calculate the direction angle φ_{11} at different θ and b. The results are presented in Fig. 5(c). At high θ, φ_{11} decreases with b, while at low θ the opposite is the case: φ_{11} increases with b. At moderate θ about 20°, φ_{11} stays almost unchanged with varying b. At high θ, even though the stable range of SkX is smaller, the variation of φ_{11} is larger (about 6° at $\theta = 50^\circ$). Another point we can notice is that at high b, for example, $b = 0.5$, by varying the polar angle θ from 50° to 10°, φ_{11} increases from about 91° to about 98°, then decreases to about 97°. That is say, not only the magnetic field strength but also the polar angle can effectively rotate SkX at certain conditions. When the in-plane component of a tilted magnetic field is along axes with high symmetry [10] and [11], SkX does not rotate at all; therefore, if we want to rotate SkX by varying the magnetic field strength or polar angle, the azimuthal angle should not be close to 0° or 45°.

Conclusion. In summary, we have revealed the effects of a tilted magnetic field on SkX in thin films of helimagnets. With negative exchange anisotropy considered, we find that both the azimuthal angle and the polar angle of a tilted magnetic field influence the stability of SkX. In general, a lower polar angle and lower azimuthal angle favor SkX. We also prove that at certain conditions a tilted magnetic field can rotate SkX by varying the azimuthal angle, polar angle, and magnetic field strength.

*Acknowledgments.*The work was supported by the NSFC (National Natural Science Foundation of China) through the funds 11772360, 11832019, 11572355, and Pearl River Nova Program of Guangzhou (Grant No. 201806010134).

[1] S. Mühlbauer, B. Binz, F. Jonietz, C. Pfleiderer, A. Rosch, A. Neubauer, R. Georgii, and P. Böni, Science **323**, 915 (2009).

[2] T. Adams, S. Mühlbauer, C. Pfleiderer, F. Jonietz, A. Bauer, A. Neubauer, R. Georgii, P. Böni, U. Keiderling, K. Everschor *et al.*, Phys. Rev. Lett. **107**, 217206 (2011).

[3] A. Tonomura, X. Yu, K. Yanagisawa, T. Matsuda, Y. Onose, N. Kanazawa, H. S. Park, and Y. Tokura, Nano Lett. **12**, 1673 (2012).

[4] T. Nakajima, H. Oike, A. Kikkawa, E. P. Gilbert, N. Booth, K. Kakurai, Y. Taguchi, Y. Tokura, F. Kagawa, and T.-h. Arima, Sci. Adv. **3**, e1602562 (2017).

[5] X. Yu, A. Kikkawa, D. Morikawa, K. Shibata, Y. Tokunaga, Y. Taguchi, and Y. Tokura, Phys. Rev. B **91**, 054411 (2015).

[6] X. Yu, N. Kanazawa, Y. Onose, K. Kimoto, W. Zhang, S. Ishiwata, Y. Matsui, and Y. Tokura, Nat. Mater. **10**, 106 (2011).

[7] K. Shibata, J. Iwasaki, N. Kanazawa, S. Aizawa, T. Tanigaki, M. Shirai, T. Nakajima, M. Kubota, M. Kawasaki, H. Park *et al.*, Nat. Nanotechnol. **10**, 589 (2015).

[8] G. Berruto, I. Madan, Y. Murooka, G. M. Vanacore, E. Pomarico, J. Rajeswari, R. Lamb, P. Huang, A. J. Kruchkov, Y. Togawa, T. LaGrange, D. McGrouther, H. M. Ronnow, and F. Carbone, Phys. Rev. Lett. **120**, 117201 (2018).

[9] X. Zhao, C. Jin, C. Wang, H. Du, J. Zang, M. Tian, R. Che, and Y. Zhang, Proc. Natl. Acad. Sci. USA **113**, 4918 (2016).

[10] W. Münzer, A. Neubauer, T. Adams, S. Mühlbauer, C. Franz, F. Jonietz, R. Georgii, P. Böni, B. Pedersen, M. Schmidt, A. Rosch, and C. Pfleiderer, Phys. Rev. B **81**, 041203(R) (2010).

[11] X. Yu, Y. Onose, N. Kanazawa, J. Park, J. Han, Y. Matsui, N. Nagaosa, and Y. Tokura, Nature (London) **465**, 901 (2010).

[12] H. S. Park, X. Yu, S. Aizawa, T. Tanigaki, T. Akashi, Y. Takahashi, T. Matsuda, N. Kanazawa, Y. Onose, D. Shindo *et al.*, Nat. Nanotechnol. **9**, 337 (2014).

[13] S. Seki, X. Yu, S. Ishiwata, and Y. Tokura, Science **336**, 198 (2012).

[14] S. Seki, J.-H. Kim, D. S. Inosov, R. Georgii, B. Keimer, S. Ishiwata, and Y. Tokura, Phys. Rev. B **85**, 220406(R) (2012).

[15] S. L. Zhang, G. van der Laan, W. W. Wang, A. A. Haghighirad, and T. Hesjedal, Phys. Rev. Lett. **120**, 227202 (2018).

[16] R. Tolley, S. Montoya, and E. Fullerton, Phys. Rev. Mater. **2**, 044404 (2018).

[17] A. Soumyanarayanan, M. Raju, A. G. Oyarce, A. K. Tan, M.-Y. Im, A. P. Petrović, P. Ho, K. Khoo, M. Tran, C. Gan *et al.*, Nat. Mater. **16**, 898 (2017).

[18] W. Jiang, G. Chen, K. Liu, J. Zang, S. G. te Velthuis, and A. Hoffmann, Phys. Rep. **704**, 1 (2017).

[19] F. Jonietz, S. Mühlbauer, C. Pfleiderer, A. Neubauer, W. Münzer, A. Bauer, T. Adams, R. Georgii, P. Böni, R. A. Duine *et al.*, Science **330**, 1648 (2010).

[20] X. Yu, N. Kanazawa, W. Zhang, T. Nagai, T. Hara, K. Kimoto, Y. Matsui, Y. Onose, and Y. Tokura, Nat. Commun. **3**, 988 (2012).

[21] X. Zhang, M. Ezawa, and Y. Zhou, Sci. Rep. **5**, 9400 (2015).

[22] X. Zhang, G. Zhao, H. Fangohr, J. P. Liu, W. Xia, J. Xia, and F. Morvan, Sci. Rep. **5**, 7643 (2015).

[23] M. Mochizuki, X. Yu, S. Seki, N. Kanazawa, W. Koshibae, J. Zang, M. Mostovoy, Y. Tokura, and N. Nagaosa, Nat. Mater. **13**, 241 (2014).

[24] A. Chacon, A. Bauer, T. Adams, F. Rucker, G. Brandl, R. Georgii, M. Garst, and C. Pfleiderer, Phys. Rev. Lett. **115**, 267202 (2015).

[25] J. S. White, K. Prša, P. Huang, A. A. Omrani, I. Živković, M. Bartkowiak, H. Berger, A. Magrez, J. L. Gavilano, G. Nagy, J. Zang, and H. M. Rønnow, Phys. Rev. Lett. **113**, 107203 (2014).

[26] S.-Z. Lin and A. Saxena, Phys. Rev. B **92**, 180401(R) (2015).

[27] C. Wang, H. Du, X. Zhao, C. Jin, M. Tian, Y. Zhang, and R. Che, Nano Lett. **17**, 2921 (2017).

[28] M. Ikka, A. Takeuchi, and M. Mochizuki, Phys. Rev. B **98**, 184428 (2018).

[29] D. Tang and Y. Qi, J. Appl. Phys. **117**, 203902 (2015).

[30] K.-W. Moon, D.-H. Kim, S.-G. Je, B. S. Chun, W. Kim, Z. Qiu, S.-B. Choe, and C. Hwang, Sci. Rep. **6**, 20360 (2016).

[31] C. Heo, N. S. Kiselev, A. K. Nandy, S. Blügel, and T. Rasing, Sci. Rep. **6**, 27146 (2016).

[32] S. Zhang, W. Wang, D. Burn, H. Peng, H. Berger, A. Bauer, C. Pfleiderer, G. van der Laan, and T. Hesjedal, Nat. Commun. **9**, 2115 (2018).

[33] S.-Z. Lin, A. Saxena, and C. D. Batista, Phys. Rev. B **91**, 224407 (2015).

[34] T. Kurumaji, T. Nakajima, V. Ukleev, A. Feoktystov, T.-h. Arima, K. Kakurai, and Y. Tokura, Phys. Rev. Lett. **119**, 237201 (2017).

[35] A. O. Leonov and I. Kézsmárki, Phys. Rev. B **96**, 014423 (2017).

[36] A. O. Leonov and I. Kézsmárki, Phys. Rev. B **96**, 214413 (2017).

[37] I. Kézsmárki, S. Bordács, P. Milde, E. Neuber, L. Eng, J. White, H. M. Rønnow, C. Dewhurst, M. Mochizuki, K. Yanai *et al.*, Nat. Mater. **14**, 1116 (2015).

[38] D. Ehlers, I. Stasinopoulos, V. Tsurkan, H.-A. Krug von Nidda, T. Fehér, A. Leonov, I. Kézsmárki, D. Grundler, and A. Loidl, Phys. Rev. B **94**, 014406 (2016).

[39] P. Padmanabhan, F. Sekiguchi, R. B. Versteeg, E. Slivina, V. Tsurkan, S. Bordács, I. Kézsmárki, and P. H. M. van Loosdrecht, Phys. Rev. Lett. **122**, 107203 (2019).

[40] S. Bordács, A. Butykai, B. Szigeti, J. White, R. Cubitt, A. Leonov, S. Widmann, D. Ehlers, H.-A. K. von Nidda, V. Tsurkan *et al.*, Sci. Rep. **7**, 7584 (2017).

[41] Y. Hu, Commun. Phys. **1**, 82 (2018).

[42] X. Wan, Y. Hu, and B. Wang, Phys. Rev. B **98**, 174427 (2018).

[43] Y. Hu and X. Wan, arXiv:1905.02165 (2019).